The influence of boron doping in the growth of ultra/nanocrystalline diamond films

Fernando A. Souza, Adriana F. Azevedo, Maurício R. Baldan and Neidenêi G. Ferreira
Instituto Nacional de Pesquisas Espaciais – INPE, Av. dos Astronautas 1758, Jd. da Granja, São José dos Campos, SP/12245-970, Brazil.

ABSTRACT

Boron-doped nanocrystalline diamond (BDND) films were grown on silicon substrates by hot filament chemical vapor deposition in $Ar/H_2/CH_4$ gas mixtures. The boron source was obtained from an additional H_2 line passing through a bubbler containing B_2O_3 dissolved in methanol with different B/C ratios. The transition from ultrananocrystalline to nanocrystalline diamond films is clearly shown by the addition of boron dopant to the growth gas mixture. The morphology and structure of these films have markedly different properties. The top view and the cross section of the films were characterized by scanning electron microscopy showing the transition from ultrananocrystalline growth (renucleation process) to a columnar structure of NCD films. Finally, the grain size was obtained from X-ray diffraction patterns of the films. The diamond average grain size increased from 10 to 35 nm for films with 2000 and 30,000 ppm B/C, respectively.

INTRODUCTION

According to the literature [1-2], ultrananocrystalline diamond (UNCD) and nanocrystalline diamond (NCD) are two different forms of diamond with unique structural properties and applications. UNCD films are generally grown in argon-rich plasma, hydrogen-poor CVD environments and NCD in hydrogen-rich growth environments [2]. However, UNCD and NCD have very different crystalline microstructures. In their work, Williams et al. [1] have reported that UNCD is a fine grain material grown at a high renucleation rate, and hence does not grow in the standard van der Drift regime. The resulting film has grain sizes smaller than 10 nm, surrounded by a layer of non-diamond carbon connecting the grains, and it presents a significant (up to 5%) sp^2-bonded carbon content. There is no columnar structure. As for the NCD, it is a thin film grown with a high first nucleation density and in the van der Drift regime. Thus, its grain size increased with the film thickness. It is accepted that NCD consists of facets smaller than 100 nm with low to moderate amounts of sp^2-bonded carbon trapped at defects or grain boundaries. During the growth process, there is little or no renucleation of the grains.

The doping of NCD and UNCD is also interesting because of the possibility of impurity incorporation and dopant electronic states associated with the grain boundaries, as well as with the bulk lattice of each grain. Wang et al. [3] have reported an investigation of the electrochemical properties of boron-doped ultrananocrystalline diamond (BDUND) and boron-doped nanocrystalline diamond (BDND) films. They concluded that, despite the morphological and structural distinctions, these films have comparable electrical and electrochemical properties that are dominated by the boron which was inserted into the diamond grains replacing the carbon. In addition, the sp^2 carbon in the grain boundaries of the UNCD films also contributes to the electrical conductivity.

In this context, the aim of this work is to show the possibility of achieving a transition from ultrananocrystalline to nanocrystalline diamond films by adding boron dopant to the growth gas mixture ($Ar/CH_4/H_2$) using the HFCVD reactor. The morphology and structure of these films were related to the boron doping level, which will be presented below.

EXPERIMENTAL DETAILS

The diamond films depositions were performed with the HFCVD technique using the following growth parameters: temperature of 900 K, pressure of 6.7 kPa, 16-hour deposition time and gas mixture of $CH_4/H_2/Ar$ with flow of 1/19/80 sccm. All the films were grown on polished silicon (100) 1x1 cm^2 samples. The boron doping was performed by the addition of B_2O_3 to the CH_3OH in the bubbler. When B_2O_3 is dissolved in CH_3OH, trimethylborate $(CH_3O)_3B$ is produced, which is probably the substance containing boron that is added to the gas mixture during the growth process. Several solutions were prepared with different concentrations of B_2O_3 dissolved in CH_3OH of 2,000, 5,000, 10,000, 20,000 and 30,000 ppm of boron atoms in relation to the carbon atoms of the CH_3OH (B/C ratios). The volume of CH_3OH was fixed at 200 mL for all solutions. These boron doping levels correspond to the acceptor density values that varied from 10^{20} to 10^{21} $B.cm^{-3}$ as the doping level increased evaluated by Raman spectra (not shown). Each solution was placed in a bubbler at a constant pressure and temperature, and the H_2 gas was used as a carrier with a constant flow of 30 sccm. The morphology and quality of the films were evaluated by scanning electron microscopy (SEM) using a JEOL JSM-5310 model, and by micro-Raman scattering spectroscopy (Renishaw microscope system 2000) using the 514.5 nm line of an argon ion laser taking the spectra covering the range from 300 to 3500 cm^{-1}. The crystallinity and the grain size of the films were investigated by X-ray diffraction (XRD) using a high resolution Philips diffractometer, X'Pert model, with the CuKα1 radiation (λ=1.54 Å) in grazing incident mode with an incident angle of 5°.

DISCUSSION

The morphology and the structure of the films were analyzed in the whole range of the boron doping levels between 2,000 and 30,000 ppm. According to the SEM images, the surface analysis of boron-doped diamond films showed a variation of surface morphology as a function of doping levels, Figs.1a-c.

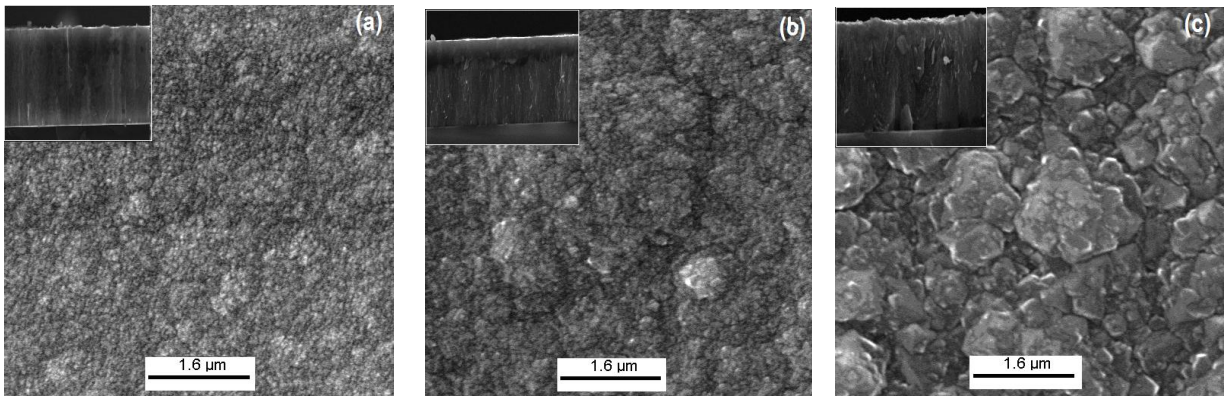

Figure. 1. SEM topographic images of BDUND and BDND films as a function of boron doping levels increased: (a) 2,000, (b) 10,000, (c) 30,000 ppm. Inset: Cross sections of these films.

The film grown with 2,000 ppm presented a uniform morphology and a flat surface while the films obtained with 5,000 and 10,000 ppm had a cauli-flower structure composed of clusters of small particles with different sizes. On the other hand, the films with high doping levels (20,000 and 30,000 ppm) presented clusters around 1.0 um composed of crystallites of different sizes. Apparently, these morphological differences are related to the growth structure as observed at inset of Figs.1a-c. The cross section images of these films showed that, for the films with low doping (2,000 ppm), there is no evidence of a columnar growth structure similar to those for the UNCD films. On the other hand, in the films doped over 10,000 ppm, the columnar structure is clear, with grain sizes increasing with distance from the substrate similar to NCD films [1].

The Raman measurements are in good agreement with the morphological changes presented by the SEM analyses. Eight features were identified in the Raman spectra of the films shown in Fig.2. The spectra for the films with low doping (< 5,000 ppm) did not have a prominent diamond one-phonon line at 1332 cm^{-1} as it is verified for single crystal diamond, of which the peak was hidden by the strong scattering of sp^2 carbon components in these films. Besides, the broadening of this peak, related to the D band present at 1350 cm^{-1}, overlapped the diamond peak. This behavior is usually noted in UNCD using Raman excitation in the visible region [1]. On the other hand, as the doping level increased, the diamond peak was visible and shifted to a lower wavenumber (1300 cm^{-1}). This shift is related to impurities formed in heavily doped films showing a metal-like conductivity [4]. The shoulders at 1150 cm^{-1} and 1490 cm^{-1} related to transpolyacetylene (TPA) segments at the grain boundaries of the NCD surface [5] tended to disappear as the doping increased. Moreover, in the film spectra with low doping (< 5,000 ppm), the peak at 1490 cm^{-1} was more intense than the G peak (1550 cm^{-1}) showing the high part of sp^2-bonded carbon in these films. This behavior was also confirmed by the high intensity of its second order Raman spectra around 2800 cm^{-1}.

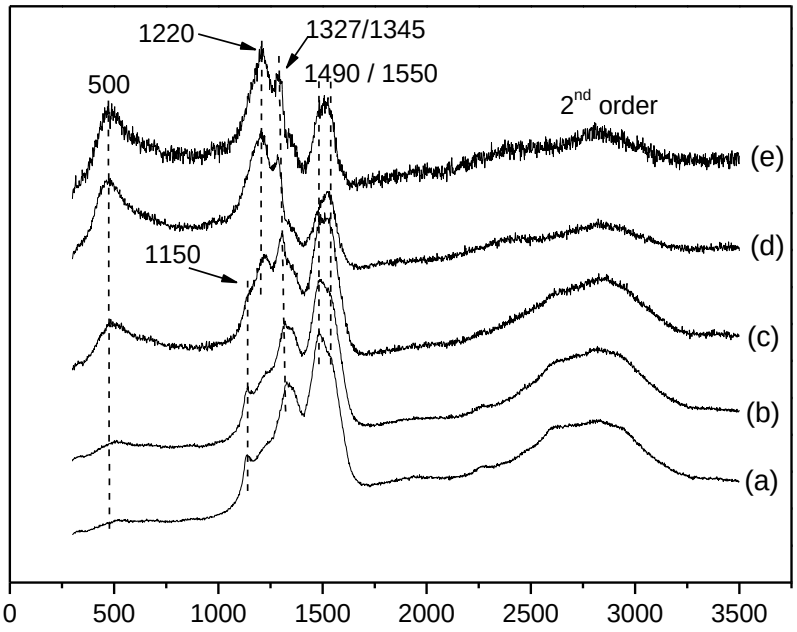

Figure 2. Raman spectra of BDUND and BDND films as a function of boron doping levels increased: (a) 2,000, (b) 5,000, (c) 10,000, (d) 20,000 and (e) 30,000 ppm.

The broad bands around 500 and 1220 cm^{-1}, which are present in the films as the doping increased, are still subject of an intense debate. They have been associated with the boron incorporation in the lattice, rather than in the number of holes of the film bulk. The presence of the 500 cm^{-1} peak is assigned to the increase in the number of boron pairs. These boron pairs have local vibration modes giving wide bands around of 500 cm^{-1} [6]. In addition, the band centered at 1220 cm^{-1} is attributed to the Fano interference between the discrete phonon state and the electronic continuum. Pruvost and Deneuville [7] have suggested the Fano effect appears above a critical percolation threshold for the achievement of the metallic conductivity on the boron impurity band. Recently, May et al. [8] have systematically studied the behavior of these bands in doped diamond films: microcrystalline, cauli-flower and faceted nanocrystalline, using different doping levels. They concluded that the band at 1220 cm^{-1} is less prominent for NCD films that present cauli-flower morphology than those that present faceted morphology. The reason is that the majority of the B is present at sites that do not contribute to the continuum of electronic states. Such sites must include interstitials, crystallite surfaces, or non-diamond carbon impurities present at the grain boundaries. This behavior may justify the low intensity of the band at 1220 cm^{-1} noted in Raman spectra of electrodes UNCD.

The XRD patterns of films are shown in Fig.3. The XRD spectra of the films deposited with 20,000 and 30,000 ppm were dominated by the peaks at 43.9°, 75.3° and 91.5° corresponding to the <111>, <220> and <311> diamond diffraction peaks that confirm the presence of crystalline diamond [9].

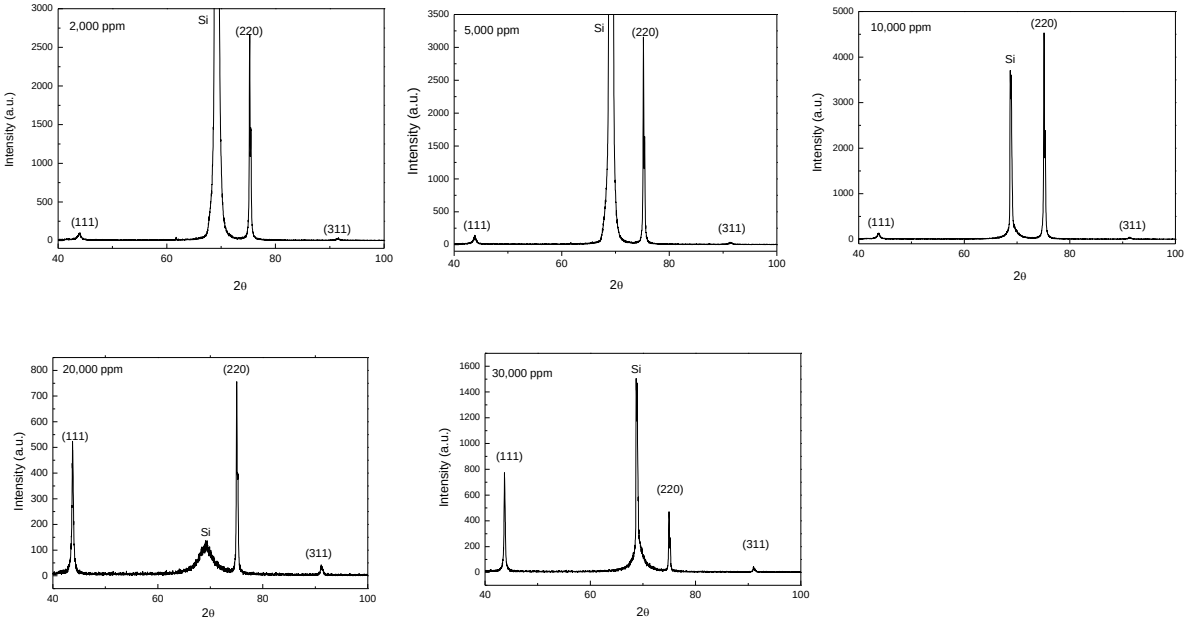

Figure 3. XRD patterns of BDUND and BDND films as a function of boron doping levels increased.

However, the <311> peak intensity was very weak compared to the other peaks. It was also observed that the <111> peak was less intense in the films grown with doping level lower than 10,000 ppm. On the other hand, the high intensity of the <220> peak in these films has been

reported as a sign of the existence of high non-diamond phase, which agrees with the Raman spectra presented in Fig.2 [10].

Some authors have used the Sherrer's equation to get the crystal size from the most intense diffraction peak, i.e. <111> [11-12]. The crystal size (L_{111}) calculated versus doping level increased from 10 to 35 nm when the doping level increased from 2,000 to 30,000 ppm. This tendency was coherent with previous observations from SEM images where the crystallite size changed from UNCD to NCD. It is important to point out that the crystallite size, calculated from line broadening of XRD peaks, and may be strongly affected by the crystal defect density [12].

CONCLUSIONS

According to the SEM images the morphology of boron-doped diamond films varied from UNCD to NCD as the boron doping levels increased. All the features in the Raman spectra of nanocrystalline diamond films were found, including the broad band around 500 cm^{-1} that correspond to the boron pair vibration. The film disorder related to graphitic compounds was analyzed from I_D/I_G ratio and decreased as the doping level increased. The XRD characterizations presented diffraction peaks of crystalline diamond in all films. Based on Sherre's equation, the diamond crystal size increased from 10 to 35 nm as the boron doping levels increased.

ACKNOWLEDGEMENTS

Special thanks to FAPESP, CAPES and CNPq for the financial support and Mrs. Maria Lúcia Brison de Mattos by the SEM analysis.

REFERENCES

1. O.A. Williams, M. Daenena, J. D'Haen, K. Haenen, J. Maes, V.V. Moshchalkov, M. Nesládek and D.M. Gruen, *Diamond Relat. Mater.* **15**, 654 (2006).
2. J.E. Butler and A.V. Sumant, *Chem. Vap. Deposition* **14,** 145 (2008).
3. S. Wang, V.M. Swope, J.E. Butler, T. Feygelson and G.M. Swain, *Diamond Relat. Mater.* **18**, 669 (2009).
4. C. Lévy-Clément, N.A. Ndao, A. Katty, M. Bernard, A. Deneuville, C. Comninellis and A. Fujishima, *Diamond Relat. Mater.* **12**, 606 (2003).
5. A.C. Ferrari and J. Robertson, *Philos. Trans. Roy. Soc. Lond. A* **362**, 2477 (2004).
6. M.Bernard, A.Deneuville and P.Muret., *Diamond Relat. Mater.* **13**, 282 (2004).
7. F. Pruvost and A. Deneuville, *Diamond Relat. Mater.* **10**, 531 (2001).
8. P.W. May, W.J. Ludlow, M. Hannaway, P.J. Heard, J.A. Smith and K.N. Rosser, *Diamond Relat. Mater.* **17**, 105 (2008).
9. A.F. Azevedo, S.C. Ramos, M.R. Baldan and N.G. Ferreira, *Diamond Relat. Mater.* **17**, 1137 (2008).
10. M.S. Haque, H.A. Naseem, A.P. Malshe, W.D. Brown, Chem. Vap. Depos. **3**, 129 (1997).

11. G. Cicala, P. Bruno, F. Bénédic, F. Silva, K. Hassouni and G.S. Senesi, *Diamond Relat. Mater.* **14**, 421 (2005).
12. K.L. Ma, W.J. Zhang, Y.S. Zou, Y.M. Chong, K.M. Leung, I. Bello and S.T. Lee, *Diamond Relat. Mater.* 15, 626 (2006).